Reflection and refraction of thermoelastic plane waves at an interface between two thermoelastic media without energy dissipation

RAJNEESH KUMAR, PARTH SARTHI

Dept. of Mathematics, Kurukshetra University,
Kurukshetra – 136 119 (India)

THE REFLECTION AND REFRACTION of thermoelastic plane waves at an imperfect interface between two dissimilar thermoelastic solid half-spaces has been investigated. The thermoelastic theory without energy dissipation developed by GREEN and NAGHDI [18] has been used to study the problem. The amplitude ratios of various reflected and refracted waves are obtained for an imperfect boundary. Particular cases of normal stiffness, transverse stiffness, slip and welded boundaries are discussed. The amplitude ratios are also deduced at the interface of two semi-infinite media (i) Elastic/Thermoelastic without energy dissipation, (ii) Thermal Conducting Liquid/Thermoelastic without energy dissipation, (iii) Non-viscous Fluid/Thermoelastic without energy dissipation, (iv) Thermal Conducting Liquid/Thermal Conducting Liquid and (v) Elastic/Elastic. It is found that the amplitude ratios of various reflected and refracted waves are affected by the stiffness and thermal properties of the media. The amplitude ratios of reflected waves are also deduced for a special case of stress-free boundary.

Key words: thermoelasticity without energy dissipation, reflection and transmission coefficients, imperfect boundary.

Notations

$\lambda\,\mu$ Lamé's constants (material constants),

ρ density of the medium,

C^* specific heat at constant strain,

t time,

T absolute temperature,

T_o the initial uniform temperature,

$u,\,w$ components of displacement vector $\mathbf{u}$,

τ_{ij} components of stress tensor,

ν a thermal parameter $= (3\lambda + 2\mu)\,\alpha_t$,

α_t coefficient of linear thermal expansion,

K^* material constant characteristics,

δ_{ij} kroneckar delta,

Δ^2 Laplace operator.

1. Introduction

There are two classical elastic boundary conditions for a solid/solid interface. One boundary condition is for the welded or perfectly bonded interface, which implies continuity of stress and displacement across the interface. The other is the slip boundary condition, which implies continuity of the normal components of stress and displacement across the interface, vanishing of the shear components of stress and discontinuity of the shear components of displacement. Physically, such a boundary condition corresponds to an infinitely thin layer of ideal liquid that ensures free transverse slip on the interface. Classical boundary conditions idealize actual physical contact between two solids and, in most cases, give excellent approximation and are supported by experimental results.

An actual interface between two solids is much more complicated and has physical properties different from those of substrates. For example, even grain boundaries in polycrystalline materials are not perfect because of misfit of the atomic structures of two neighboring grains. In this case dislocation may form on the interface and the atomic structure becomes different than in the bulk medium. This interface imperfection may be detected only at very high frequencies. Another example of formation of a thin interface layer occurs when two solids are bonded together either by a thin layer of other materials, for example, glue or by some metallurgical process. Depending on the properties of this layer, what has been demonstrated by Rokhlin and Marom [15], the boundary between the solids may behave as slip, perfect or neither and its state significantly affects elastic wave reflection and interface mechanical behavior.

Significant work has been done to describe the physical conditions on the interface due to different mechanical boundary conditions due to different investigators. Notable among them are Jones and Whittier [4]; Murty [8]; Nayfeh and Nassar [9]; Rokhlin et al. [10]; Rokhlin [12]; Pilarski and Rose [16].

Baik and Thomson [13] took an important step to describe physically the interface stiffness; they introduced a new quasi-static model that define the interface stiffness using the known static solution for an elastic body with cracks. The problem of elastic wave diffraction by interface imperfection was studied by Achenbach and coauthors [14]. Lovrentyev and Rokhlin [21] investigated the imperfect boundary conditions between two elastic solid half-spaces.

Thermoelasticity theories which admit a finite speed of thermal signals (second sound) have attracted much interest in the last four decades. In contrast to the conventional coupled thermoelasticity theory (CTE) based on a par-

abolic heat equation, which predicts an infinite speed for the propagation of heat, these theories involve a hyperbolic heat equation and are referred to as generalized thermoelasticity theories. Among these generalized theories, the extended thermoelasticity theory (ETE) proposed by LORD and SHULMAN [3] and temperature rate-dependent thermoelasticity theory developed by GREEN and LINDSAY [5] have been subjected to a large number of investigations. In view of the experimental evidence available in favor of finiteness of the heat propagation speed, generalized thermoelasticity theories are considered to be more realistic than the conventional thermoelasticity theory in dealing with practical problems involving very large heat fluxes at short intervals, like those occurring in laser units and energy channels.

Recently GREEN and NAGHDI [18], proposed a new thermoelasticity theory by including the 'thermal-displacement gradient' among the independent constitutive variables. An important feature of this theory which is not present in other thermoelasticity theories is that this theory does not accommodate dissipation of thermal energy.

DERESIEWICZ [1] studied the reflection of a plane wave from a plane stress-free boundary in coupled theory of thermoelasticity and investigated the effect of boundaries on these waves. But there is some algebraic mistake in the expressions for the amplitude ratios, which was corrected by him in 1962 [2]. The reflection of thermoelastic waves at a solid half-space with one relaxation time was investigated by SINHA and SINHA [6]. BEEVERS and BREE [7] discussed a wave reflection problem in linear coupled thermoelasticity. SHARMA [17] discussed the reflection of thermoelastic waves from the stress-free insulated boundary of anisotropic half-space. SINHA and ELSIBAI [19] studied the effect of two relaxation times on the reflection of thermoelastic waves at a homogeneous, isotropic and thermal conducting elastic solid half-space. SINHA and ELSIBAI [20] studied also the reflection and refraction of thermoelastic waves at an interface of two semi-infinite media in contact, with two relaxation times. SINGH and KUMAR [22, 23] investigated the reflection of plane waves from the flat boundary of a micropolar generalized thermoelastic half-space and micropolar generalized thermoelastic half-space with stretch. SINGH and KUMAR [24] also investigated the wave propagation in generalized thermo-microstretch elastic solid. ABD-ALLA and AL-DAWY [25] discussed the reflection of thermoelastic plane wave at a generalized thermoelastic half-space with one and two relaxation times. SINGH [26] investigated the plane wave propagation in a homogeneous transversally isotropic thermo-coupled elastic solid. SINGH [27] discussed the reflection of plane wave from the free surface of a viscous thermoelastic half-space.

The present investigation is concerned with the reflection and transmission of thermoelastic plane waves in a thermoelastic medium without energy dissipation and various special cases have been deduced.

2. Formulation of the problem and basic equations

We consider two homogeneous isotropic thermoelastic solids without energy dissipation being in contact with each other at a plane surface, which we denote as the plane $z = 0$ of a rectangular co-ordinate system $OXYZ$. We consider thermoelastic plane waves in the xz-plane with wave front parallel to y-axis and all the field variables depend only on x, z and t.

Following GREEN and NAGHDI [18], the field equations of the thermoelastic solid without energy dissipation in absence of body forces and heat sources and the constitutive relations can be written as

$$(2.1) \qquad (\lambda + \mu) \nabla (\nabla.\mathbf{u}) + \mu \nabla^2 \mathbf{u} - \nu \nabla T = \rho \frac{\partial^2 \mathbf{u}}{\partial t^2},$$

$$(2.2) \qquad K^* \nabla^2 T = \rho C^* \frac{\partial^2 T}{\partial t^2} + \nu T_o \frac{\partial^2}{\partial t^2} \nabla.\mathbf{u}.$$

The stress-displacement and temperature relations are

$$(2.3) \qquad \tau_{ij} = \lambda u_{r,r} \delta_{ij} + \mu (u_{i,j} + u_{j,i}) - \nu T \delta_{ij}.$$

The list of the symbols is given at the beginning of the paper. For a two-dimensional problem, the displacement vector $\mathbf{u}$ is taken as

$$(2.4) \qquad \mathbf{u} = (u,\ 0,\ w),$$

where the displacement components u and w are related by the potential functions ϕ and ψ as

$$(2.5) \qquad \begin{aligned} u &= \frac{\partial \phi}{\partial x} - \frac{\partial \psi}{\partial z}\ , \\ w &= \frac{\partial \phi}{\partial z} + \frac{\partial \psi}{\partial x}\ . \end{aligned}$$

Substituting the values of u and w from Eq. (2.5) in Eqs. (2.1), (2.2) with the help of (2.4), we obtain

$$(2.6) \qquad c_1^2 \nabla^2 \phi - \bar{\nu} T = \frac{\partial^2 \phi}{\partial t^2},$$

$$(2.7) \qquad c_2^2 \nabla^2 \psi = \frac{\partial^2 \psi}{\partial t^2},$$

$$(2.8) \qquad \overline{K}^* \nabla^2 T = C^* \frac{\partial^2 T}{\partial t^2} + \bar{\nu}\, T_o \frac{\partial^2}{\partial t^2} \left(\nabla^2 \phi \right),$$

where

$$c_1^2 = \frac{\lambda + 2\mu}{\rho}; \qquad c_2^2 = \frac{\mu}{\rho}; \qquad \bar{\nu} = \frac{\nu}{\rho}; \qquad \overline{K}^* = \frac{K^*}{\rho}.$$

From Eqs. (2.6)–(2.8), we observe that while P-wave is affected by the presence of the T-wave and *vice versa*, the SV-wave remains unaffected.

Substituting the value of T from (2.6) in (2.8), we obtain

$$(2.9) \qquad \nabla^4\phi - \nabla^2 \left[\frac{1}{c_1^2} + \frac{C^*}{\overline{K}^*}(1+\varepsilon)\right] \frac{\partial^2\phi}{\partial t^2} + \frac{C^*}{\overline{K}^* c_1^2} \frac{\partial^4\phi}{\partial t^4} = 0,$$

where

$$\varepsilon = \frac{\bar{\nu}^2 T_o}{C^* c_1^2}.$$

To solve Eqs. (2.7) and (2.9), we assume

$$(2.10) \qquad \phi \sim \phi\, e^{-i\omega t}, \qquad T \sim T\, e^{-i\omega t}, \qquad \psi \sim \psi\, e^{-i\omega t}.$$

With the help of Eq. (2.10), Eq. (2.9) reduces to

$$(2.11) \qquad \nabla^4\phi + A\omega^2\nabla^2\phi + B\omega^4\phi = 0,$$

where

$$A = \frac{1}{c_1^2} + \frac{C^*}{\overline{K}^*}(1+\varepsilon), \qquad B = \frac{C^*}{\overline{K}^* c_1^2}.$$

We assume the solution of Eq. (2.11) as

$$(2.12) \qquad \phi = \phi_1 + \phi_2,$$

where ϕ_1 and ϕ_2 satisfy

$$(2.13) \qquad \begin{aligned} (\nabla^2 + \delta_1^2)\,\phi_1 &= 0, \\ (\nabla^2 + \delta_2^2)\,\phi_2 &= 0, \end{aligned}$$

and where

$$\delta_1^2 = \omega^2\lambda_1^2, \qquad \delta_2^2 = \omega^2\lambda_2^2,$$

with

$$\lambda_1 = \left[\frac{1}{2}\left(\sqrt{A^2 - 4B} + A\right)\right]^{1/2}, \qquad \lambda_2 = \left[\left(\frac{1}{2}\right)\left(-\sqrt{A^2 - 4B} + A\right)\right]^{1/2}.$$

From Eq. (2.6), we obtain

$$(2.14) \qquad T = a_1\phi_1 + a_2\phi_2,$$

where

$$a_i = \frac{1}{\nu}\left(-\delta_i^2 c_1^2 + \omega^2\right), \qquad (i = 1, \ 2).$$

Similarly Eq. (2.7) with the help of Eq. (2.10) takes the form

(2.15) $$\left(\nabla^2 + \delta_3^2\right)\psi = 0,$$

where

$$\delta_3^2 = \frac{\omega^2}{c_2^2}.$$

3. Reflection and transmission

We consider a thermoelastic plane wave (P- or SV- or T-) propagating through the medium M, which we identify as the region $z > 0$ and fallingat the plane $z = 0$, with its direction of propagation making an angle θ_o with the normal to the surface. Corresponding to each incident wave, we get the waves in medium M as reflected P-, SV- and T- waves and transmitted P-, SV- and T- waves in the medium M'. We write all the variables without the primes in the region $z > 0$ (medium M) and attach a prime to denote the variables in the region $z < 0$ (medium M'), as shown in Fig. 1.
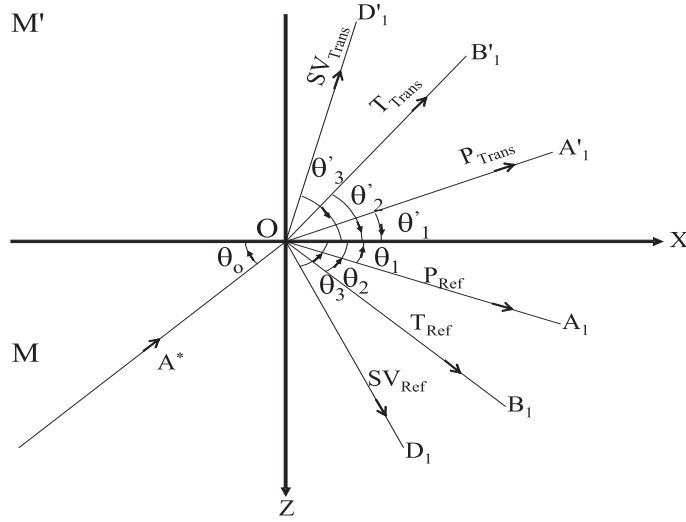
Fig. 1. Geometry of the problem.

4. Imperfect boundary conditions

We consider a two-bonded homogenous isotropic thermoelastic solids in contact, as shown in Fig. 1. If the bonding is imperfect and the size and spacing between the imperfection is much smaller than the wavelength, then at the interface these can be described by using spring boundary condition (LAVRENTYEV and ROKHLIN [21]), i.e. at $z = 0$

$$\tau'_{33} = K_n \left[w - w' \right],$$
$$\tau'_{31} = K_t \left(u - u' \right),$$
$$K^{*'} \frac{\partial T'}{\partial z} = K_c (T - T'),$$
$$\tau'_{33} = \tau_{33},$$
$$\tau'_{31} = \tau_{31},$$
$$K^{*'} \frac{\partial T'}{\partial z} = K^* \frac{\partial T}{\partial z},$$

(4.1)

where K_n and K_t are normal and transverse stiffness coefficients of a unit layer thickness and have dimension N/m^3, and K_c is the thermal contact conductance with dimension W/m^2 K sec.

The appropriate potentials satisfying the boundary conditions are

Medium M:

(4.2) $\quad \phi = A_0 \exp \left\{ i\delta_1 \left(x \cos \theta_0 - z \sin \theta_0 \right) - i\omega_1 t \right\}$

$$+ A_1 \exp \left\{ i\delta_1 \left(x \cos \theta_1 + z \sin \theta_1 \right) - i\omega_1 t \right\},$$
$$+ B_0 \exp \left\{ i\delta_2 \left(x \cos \theta_0 - z \sin \theta_0 \right) - i\omega_2 t \right\}$$
$$+ B_1 \exp \left\{ i\delta_2 \left(x \cos \theta_2 + z \sin \theta_2 \right) - i\omega_2 t \right\},$$

(4.3) $\quad T = a_1 A_0 \exp \left\{ i\delta_1 \left(x \cos \theta_0 - z \sin \theta_0 \right) - i\omega_1 t \right\}$

$$+ a_1 A_1 \exp \left\{ i\delta_1 \left(x \cos \theta_1 + z \sin \theta_1 \right) - i\omega_1 t \right\}$$
$$+ a_2 B_0 \exp \left\{ i\delta_2 \left(x \cos \theta_0 - z \sin \theta_0 \right) - i\omega_2 t \right\}$$
$$+ a_2 B_1 \exp \left\{ i\delta_2 \left(x \cos \theta_2 + z \sin \theta_2 \right) - i\omega_2 t \right\},$$

(4.4) $\quad \psi = D_0 \exp \left\{ i\delta_3 (x \cos \theta_0 - z \sin \theta_0) - i\omega_3 t \right\}$

$$+ D_1 \exp \left\{ i\delta_3 (x \cos \theta_3 + z \sin \theta_3) - i\omega_3 t \right\}.$$

Medium M′:

(4.5) $\qquad \phi' = A_1' \exp\left\{i\delta_1'\left(x\cos\theta_1' - z\sin\theta_1'\right) - i\omega_1' t\right\}$

$$+ B_1' \exp\left\{i\delta_2'\left(x\cos\theta_2' - z\sin\theta_2'\right) - i\omega_2' t\right\},$$

(4.6) $\qquad T' = a_1' A_1' \exp\left\{i\delta_1'\left(x\cos\theta_1' - z\sin\theta_1'\right) - i\omega_1' t\right\}$

$$+ a_2' B_1' \exp\left\{i\delta_2'\left(x\cos\theta_2' - z\sin\theta_2'\right) - i\omega_2' t\right\},$$

(4.7) $\qquad \psi' = D_1' \exp\left\{i\delta_3'(x\cos\theta_3' - z\sin\theta_3') - i\omega_3' t\right\},$

where

$\qquad B_0, D_0 = 0, \quad$ for incident P-wave,

$\qquad A_0, B_0 = 0, \quad$ for incident SV-wave,

$\qquad A_0, D_0 = 0, \quad$ for incident T-wave.

Snell's law is given as

(4.8) $\qquad \dfrac{\cos\theta_0}{V_0} = \dfrac{\cos\theta_1}{\lambda_1^{-1}} = \dfrac{\cos\theta_2}{\lambda_2^{-1}} = \dfrac{\cos\theta_3}{\lambda_3^{-1}} = \dfrac{\cos\theta_1'}{(\lambda_1')^{-1}} = \dfrac{\cos\theta_2'}{(\lambda_2')^{-1}} = \dfrac{\cos\theta_3'}{(\lambda_3')^{-1}}$

where

(4.9) $\qquad \delta_1\left(\lambda_1^{-1}\right) = \delta_2\left(\lambda_2^{-1}\right) = \delta_3\left(\lambda_3^{-1}\right)$

$$= \delta_1'\left[\left(\lambda_1'\right)^{-1}\right] = \delta_2'\left[\left(\lambda_2'\right)^{-1}\right] = \delta_3'\left[\left(\lambda_3'\right)^{-1}\right] \qquad \text{at} \quad z = 0,$$

and

(4.10) $\qquad V_0 = \begin{cases} \lambda_1^{-1}, & \text{for incident } P\text{-wave,} \\ \lambda_2^{-1}, & \text{for incident } T\text{-wave,} \\ \lambda_3^{-1}, & \text{for incident } SV\text{-wave.} \end{cases}$

Making use of the potentials given by Eqs. (4.2)–(4.7) in boundary conditions (4.1) and using Eqs. (2.3) and (2.5), we get a system of six non-homogeneous equations which can be written as

(4.11) $\qquad \displaystyle\sum_i^6 a_{ij} Z_j = Y_i, \qquad (j = 1, 2...6),$

where

$$a_{11} = iK_n\delta_1\,\sin\theta_1,$$

$$a_{12} = iK_n\delta_2\sin\theta_2,$$

$$a_{13} = i\,K_n\delta_3\cos\theta_3,$$

$$a_{14} = iK_n\delta_1'\sin\theta_1' + \lambda'\delta_1'^2 + \nu'a_1' + 2\mu'\delta_1'^2\sin^2\theta_1,$$

$$a_{15} = iK_n\delta_2'\sin\theta_2' + \lambda'\delta_2'^2 + \nu'a_2' + 2\mu'\delta_2'^2\sin^2\theta_2',$$

$$a_{16} = -\left(i\delta_3'K_n\cos\theta_3' + \mu'\delta_3^2\sin2\theta_3'\right),$$

$$a_{21} = iK_t\delta_1\cos\theta_1,$$

$$a_{22} = iK_t\delta_2\cos\theta_2,$$

$$a_{23} = -iK_t\delta_3\sin\theta_3,$$

$$a_{24} = -(\mu'\delta_1'^2\sin2\theta_1' + i\delta_1'K_t\cos\theta_1'),$$

$$a_{25} = -(\mu'\delta_2'^2\sin2\theta_2' + i\delta_2'K_t\cos\theta_2'),$$

$$a_{26} = \mu'\delta_3'^2\cos2\theta_3' + i\delta_3'K_t\sin\theta_3',$$

$$a_{31} = K_ca_1,$$

$$a_{32} = K_ca_2,$$

$$a_{33} = a_{36} = 0,$$

$$a_{34} = -(K_ca_1' - iK^{*'}\delta_1'a_1'\sin\theta_1'),$$

$$a_{35} = -\left(K_ca_2 - iK^{*'}\delta_2'a_2'\sin\theta_2'\right),$$

$$a_{41} = -\left(\lambda + 2\mu\sin^2\theta_1\right)\delta_1^2 - \nu\,a_1,$$

$$a_{42} = -\left(\lambda + 2\mu\sin^2\theta_2\right)\delta_2^2 - \nu\,a_2,$$

$$a_{43} = -\mu\delta_3^2\sin2\theta_3,$$

$$a_{44} = \left(\lambda' + 2\mu'\sin^2\theta_1'\right)\delta_1'^2 + \nu'\,a_1',$$

$$a_{45} = \left(\lambda' + 2\mu'\sin^2\theta_2'\right)\delta_2'^2 + \nu'\,a_2',$$

$$a_{46} = -\mu'\delta_3'^2\sin2\theta_3',$$

$$a_{51} = \mu\delta_1^2\sin2\theta_1,$$

$$a_{52} = \mu\delta_2^2\sin2\theta_2,$$

$$a_{53} = \mu\delta_3^2\cos2\theta_3,$$

$$a_{54} = \mu' {\delta'}_1^{'2} \sin 2\theta'_1,$$

$$a_{55} = \mu' {\delta'}_2^{2} \sin 2\theta'_2,$$

$$a_{56} = -\mu' {\delta'}_3^{2} \cos 2\theta'_3,$$

$$a_{61} = iK^* a_1 \delta_1 \sin \theta_1,$$

$$a_{62} = iK^* a_2 \delta_2 \sin \theta_2,$$

$$a_{64} = iK^{*'} a'_1 \delta'_1 \sin \theta'_1,$$

$$a_{65} = iK^{*'} a'_2 \delta'_2 \sin \theta'_2$$

$$a_{63} = a_{66} = 0$$

and

$$Z_1 = \frac{A_1}{A^*}; \quad Z_2 = \frac{B_1}{A^*}; \quad Z_3 = \frac{D_1}{A^*}; \quad Z_4 = \frac{A'_1}{A^*}; \quad Z_5 = \frac{B'_1}{A^*}; \quad Z_6 = \frac{D'_1}{A^*};$$

(a) For incident P-wave

$$A^* = A_0, \quad Y_1 = a_{11}, \quad Y_2 = -a_{21}, \quad Y_3 = -a_{31},$$

$$Y_4 = -a_{41}, \quad Y_5 = a_{51}, \quad Y_6 = a_{61},$$

(b) For incident SV-wave

$$A^* \equiv D_0, \quad Y_1 = -a_{13}, \quad Y_2 = a_{23}, \quad Y_3 = a_{33},$$

$$Y_4 = a_{43}, \quad Y_5 = -a_{53}, \quad Y_6 = -a_{63}.$$

(c) For incident T-wave

$$A^* \equiv \mathbf{B}_o, \quad Y_1 = a_{12}, \quad Y_2 = -a_{22}, \quad Y_3 = -a_{32},$$

$$Y_4 = -a_{42}, \quad Y_5 = a_{52}, \quad Y_6 = a_{62},$$

where Z_1, Z_2, Z_3 are the amplitude ratios of reflected P-, T- and SV-waves and Z_4, Z_5, Z_6 are the amplitude ratios of refracted P-, T-, and SV-wave, respectively.

5. Cases

CASE 1. **Normal Stiffness**

In the case $K_n \neq 0$, $K_t \to \infty$, $K_c \to \infty$, we have a boundary with normal stiffness and obtain a system of six non-homogeneous equations as given by Eq. (4.11) with changed values of a_{ij} as

$$a_{21} = i\delta_1 \cos \theta_1, \quad a_{22} = i\delta_2 \cos \theta_2, \quad a_{23} = -i\delta_3 \sin \theta_3,$$

$$a_{24} = -i\delta'_1 \cos \theta'_1, \quad a_{25} = -i\delta'_2 \cos \theta'_2, \quad a_{26} = -i\delta'_3 \sin \theta'_3,$$

$$a_{31} = a_1, \quad a_{32} = a_2, \quad a_{34} = -a_1, \quad a_{35} = -a_2.$$

CASE 2. **Transversal Stiffness**

Taking $K_n \to \infty, \; K_t \neq 0, K_c \to \infty$, the imperfect boundary reduces to the transverse stiffness and we obtain a system of six non-homogeneous equations as given by Eq. (4.11); the values of a_{ij}; take the following form:

$$a_{11} = i\delta_1 \sin \theta_1 \;, \quad a_{12} = i\delta_2 \sin \theta_2 \;, \quad a_{13} = i\delta_3 \cos \theta_3 \;,$$

$$a_{14} = i\delta_1' \sin \theta_1' \;, \quad a_{15} = i\delta_2' \sin \theta_2' \;, \quad a_{16} = -i\delta_3' \cos \theta_3',$$

$$a_{31} = a_1, \quad a_{32} = a_2, \quad a_{34} = -a_1', \quad a_{35} = -a_2'.$$

CASE 3. **Thermal Contact Conductance**

With $K_n \to \infty, \; K_t \to \infty, \; K_c \neq 0$, the imperfect boundary reduces to a thermally conducting imperfect surface, getting systems of six non-homogeneous equations as given by Eq. (4.11) and the modified values of a_{ij} are

$$a_{11} = i\delta_1 \sin \theta_1, \qquad a_{12} = i\delta_2 \sin \theta_2, \qquad a_{13} = i\delta_3 \cos \theta_3,$$

$$a_{14} = i\delta_1' \sin \theta_1', \qquad a_{15} = i\delta_2' \sin \theta_2', \qquad a_{16} = -i\delta_3' \cos \theta_3',$$

$$a_{21} = i\delta_1 \cos \theta_1, \qquad a_{22} = i\delta_2 \cos \theta_2, \qquad a_{23} = -i\delta_3 \sin \theta_3, \qquad a_{24} = -i\delta_1' \cos \theta_1',$$

$$a_{25} = -i\delta_2' \cos \theta_2', \qquad a_{26} = -i\delta_3' \sin \theta_3'.$$

CASE 4. **Welded Contact**

In this case $K_n \to \infty, \; K_t \to \infty, \; K_c \to \infty$ then we obtain a system of Eqs. (4.11) with changed values of a_{ij} as

$$a_{11} = i\delta_1 \sin \theta_1, \qquad a_{12} = i\delta_2 \sin \theta_2, \qquad a_{13} = i\delta_3 \cos \theta_3,$$

$$a_{14} = i\delta_1' \sin \theta_1', \qquad a_{15} = i\delta_2' \sin \theta_2', \qquad a_{16} = -i\delta_3' \cos \theta_3',$$

$$a_{21} = i\delta_1 \cos \theta_1, \qquad a_{22} = i\delta_2 \cos \theta_2, \qquad a_{23} = -i\delta_3 \sin \theta_3,$$

$$a_{24} = -i\delta_1' \cos \theta_1', \qquad a_{25} = -i\delta_2' \cos \theta_2', \qquad a_{26} = -i\delta_3' \sin \theta_3',$$

$$a_{31} = a_1, \qquad a_{32} = a_2, \qquad a_{34} = -a_1', \qquad a_{35} = -a_2'.$$

CASE 5. **Slip Boundary**

If $K_n \to \infty, \; K_t \to 0, K_c \to \infty$, then the imperfect boundary becomes a slip boundary and we obtain a system of six non-homogeneous equations as given by

Eqs. (4.11) with modified values of a_{ij} as

$$a_{11} = i\delta_1 \sin\theta_1, \qquad a_{12} = i\delta_2 \sin\theta_2, \qquad a_{13} = i\delta_3 \cos\theta_3$$

$$a_{14} = i\delta_1' \sin\theta_1', \qquad a_{15} = i\delta_2' \sin\theta_2', \qquad a_{16} = -i\delta_3' \cos\theta_3',$$

$$a_{21} = a_{22} = a_{23} = 0, \qquad a_{24} = \mu'\delta_1'^2 \sin 2\theta_1',$$

$$a_{25} = \mu'\delta_2'^2 \sin 2\theta_2', \qquad a_{26} = -\mu'\delta_3'^2 \cos 2\theta_3',$$

$$a_{31} = a_1, \qquad a_{32} = a_2, \qquad a_{34} = -a_1',$$

$$a_{35} = -a_2', \qquad a_{44} = a_{45} = 0 = a_{46}.$$

Special case: Stress-Free Boundary

In this case when $K_n \to 0$, $K_t \to 0$, $K_c \to \infty$ our results reduce to the stress-free thermoelastic boundary and we obtain a system of three non-homogeneous equations:

(5.1)
$$\sum_{i=1}^{3} c_{ij} Z_j = Y_i, \quad (j = 1, 2, 3),$$

where

$$c_{11} = \left(\lambda + 2\mu \sin^2\theta_1\right)\delta_1^2 + \nu a_1, \qquad c_{12} = \left(\lambda + 2\mu \sin^2\theta_2\right)\delta_2^2 + \nu a_2,$$

$$c_{13} = \mu\delta_3^2 \sin 2\theta_3, \qquad c_{21} = \mu\delta_1^2 \sin 2\theta_1,$$

$$c_{22} = \mu\delta_2^2 \sin 2\theta_2, \qquad c_{23} = \mu\delta_3^2 \cos 2\theta_3,$$

$$c_{31} = a_1, \qquad c_{32} = a_2, \qquad c_{33} = 0 \qquad \text{[Isothermal boundary]}$$

or

$$c_{31} = ia_1\delta_1 \sin\theta_1, \qquad c_{32} = ia_2\delta_2 \sin\theta_2, \qquad c_{33} = 0, \qquad \text{[Insulated boundary]}$$

with
$$Z_1 = \frac{A_1}{A^*}, \qquad Z_2 = \frac{B_1}{A^*}, \qquad Z_3 = \frac{D_1}{A^*}.$$

(a) For incident P-wave; $A^* = A_0$

$$[Y_1 = -c_{11}, \qquad Y_2 = c_{21}, \qquad Y_3 = -c_{31} \quad \text{(Isothermal)}$$

$$Y_3 = c_{31}, \qquad \text{(Insulated)}]$$

(b) For incident SV-wave, $A^* = D_0$

$$[Y_1 = c_{13}, \qquad Y_2 = -c_{23}, \qquad Y_3 = c_{33}]$$

(c) For incident T-wave, $A^* = B_0$

$$[Y_1 = -c_{12}, \qquad Y_2 = c_{22}, \qquad Y_3 = -c_{32}, \qquad \text{(Isothermal)}$$

$$Y_3 = c_{32}, \qquad \text{(Insulated)}]$$

where Z_1, Z_2 and Z_3 are the amplitude ratios of reflected P-, T- and SV- waves respectively.

6. Deductions

(A) : In absence of the thermal effect in medium M', we obtain the elastic/ thermoelastic imperfect boundary. We obtain a system of five non-homogeneous equations, which can be written as

(6.1)
$$\sum_{i=1}^{5} a_{ij} Z_j^* = Y_i^*, (j = 1, ..., 5),$$

where

$$a_{11} = iK_n\delta_1, \sin\theta_1, \qquad a_{12} = iK_n\delta_2\sin\theta_2, \qquad a_{13} = i\,K_n\delta_3\cos\theta_3,$$

$$a_{14} = iK_n\delta_1' \sin\theta_1' + \lambda'\delta_1'^2 + 2\mu'\delta_1'^2\sin^2\theta_1',$$

$$a_{15} = -\left(i\delta_3'K_n\cos\theta_3' + \mu'\delta_3'^2\sin 2\theta_3'\right),$$

$$a_{21} = iK_t\delta_1\cos\theta_1, \qquad a_{22} = iK_t\delta_2\cos\theta_2, \qquad a_{23} = -iK_t\delta_3\sin\theta_3,$$

$$a_{24} = -(\mu'\delta_1'^2\sin 2\theta_1' + i\delta_1'K_t\cos\theta_1'), \qquad a_{25} = \mu'\delta_3'^2\cos 2\theta_3' + i\delta_3'K_t\sin\theta_3',$$

$$a_{31} = -\left(\lambda + 2\mu\sin^2\theta_1\right)\delta_1^2 - \nu\,a_1, \qquad a_{32} = -\left(\lambda + 2\mu\sin^2\theta_2\right)\delta_2^2 - \nu\,a_2,$$

$$a_{33} = -\mu\delta_3^2\sin 2\theta_3 \qquad a_{34} = \left(\lambda' + 2\mu'\sin^2\theta_1'\right)\delta_1'^2 \qquad a_{35} = -\mu'\delta_3'^2\sin 2\theta_3',$$

$$a_{41} = \mu\delta_1^2\sin 2\theta_1, \qquad a_{42} = \mu\delta_2^2\sin 2\theta_2, \qquad a_{43} = \mu\delta_3^2\cos 2\theta_3,$$

$$a_{44} = \mu'\delta_1'^2\sin 2\theta_1', \qquad a_{45} = -\mu'\delta_3'^2\cos 2\theta_3',$$

$$a_{51} = a_1, \qquad a_{52} = a_2, \qquad a_{53} = a_{54} = a_{55} = 0,$$

with

$$\lambda_1'^2 = \frac{1}{c_1'^2}, \qquad \lambda_2'^2 = 0;$$

and

$$Z_1^* = \frac{A_1}{A^*}, \quad Z_2^* = \frac{B_1}{A^*}, \quad Z_3^* = \frac{D_1}{A^*}, \quad Z_4^* = \frac{A_1'}{A^*}, \quad Z_5^* = \frac{D_1'}{A^*};$$

(a) For Incident P-wave; $A^* = A_0$

$$\begin{bmatrix} Y_1^* = a_{11}, & Y_2^* = -a_{21}, & Y_3^* = -a_{31} \\ Y_4^* = a_{41}, & Y_5^* = -a_{51}, \end{bmatrix}$$

(b) For Incident SV-wave; $A^* = D_0$

$$\begin{bmatrix} Y_1^* = -a_{13}^*, & Y_2^* = a_{23}^*, & Y_3^* = a_{33}^*; \\ Y_4^* = -a_{43}^*, & Y_5^* = a_{53}^* \end{bmatrix}$$

(c) For Incident T-wave; $A^* = B_0$

$$\begin{bmatrix} Y_1^* = a_{12}^*, & Y_2^* = -a_{22}^*, & Y_3^* = -a_{32}^*, \\ Y_4^* = a_{42}^*, & Y_5^* = -a_{52}^*, \end{bmatrix}$$

where Z_1^*, Z_2^*, Z_3^* are amplitude ratios of reflected P-,T- and SV- waves and Z_4^*, Z_5^* are the amplitude ratios of transmitted P- and SV-waves respectively.

(B): Taking $\mu' \to 0$ in medium M', we obtain an interface of thermally conducting liquid/thermoelastic solid half-spaces, leading to a system of five non-homogeneous equations, which can be written as

$$\sum_{i=1}^{5} a_{ij}\, Z_j = Y_i\, , (j = 1, 2, ..., 5),$$

where

$$a_{11} = iK_n\delta_1\, \sin\theta_1, \qquad a_{12} = iK_n\delta_2\sin\theta_2, \qquad a_{13} = i\, K_n\delta_3\cos\theta_3,$$

$$a_{14} = iK_n\delta_1'\sin\theta_1' + \lambda'\delta_1'^2 + \nu'a_1', \qquad a_{15} = iK_n\delta_2'\sin\theta_2' + \lambda'\delta_2'^2 + \nu'a_2',$$

$$a_{21} = a_1, \qquad a_{22} = a_2, \qquad a_{24} = -a_1', \qquad a_{25} = -a_2', \qquad a_{23} = 0,$$

$$a_{31} = -\left(\lambda + 2\mu\sin^2\theta_1\right)\delta_1^2 - \nu\, a_1, \qquad a_{32} = -\left(\lambda + 2\mu\sin^2\theta_2\right)\delta_2^2 - \nu\, a_2,$$

$$a_{33} = -\mu\delta_3^2\sin 2\theta_3, \qquad a_{34} = \lambda'\delta_1'^2 + \nu'\, a_1', \qquad a_{35} = \lambda'\delta_2'^2 + \nu'\, a_2',$$

$$a_{41} = \mu\delta_1^2\sin 2\theta_1, \qquad a_{42} = \mu\delta_2^2\sin 2\theta_2,$$

$$a_{43} = \mu\delta_3^2\cos 2\theta_3, \qquad a_{44} = a_{45} = 0,$$

$$a_{51} = a_1\left(iK^*\delta_1\sin\theta_1 - h_c\right), \qquad a_{52} = a_2\left(iK^*\delta_2\sin\theta_2 - h_c\right),$$

$$a_{54} = h_c a_1', \qquad a_{55} = h_c a_2', \qquad a_{53} = 0,$$

where h_c is heat transfer coeffivient at the interface,

and

$$\lambda'_1 = \left[\frac{1}{2} \left(\sqrt{A'^2 - 4B'} + A' \right) \right]^{1/2},$$

(6.2)

$$\lambda'_2 = \left[\frac{1}{2} \left(-\sqrt{A'^2 - 4B'} + A' \right) \right]^{1/2},$$

where

$$A' = \frac{C^{*\prime}}{\overline{K}^{*\prime}} (1 + \varepsilon') + \frac{1}{c_1'^2},$$

$$B' = \frac{C^{*\prime}}{\overline{K}^{*\prime} c_{1^2}'},$$

$$c_1'^2 = \frac{\lambda'}{\rho'}.$$

and

$$Z_1 = \frac{A_1}{A^*}, \qquad Z_2 = \frac{B_1}{A^*}, \qquad Z_3 = \frac{D_1}{A^*}, \qquad Z_4 = \frac{A_1'}{A^*}, \qquad Z_5 = \frac{B_1'}{A^*}$$

(a) For Incident P-Wave; $A^* = A_0$

$$[Y_1 = a_{11}, \quad Y_2 = -a_{21}, \quad Y_3 = -a_{31}, \quad Y_4 = a_{41}, \quad Y_5 = a_{51}]$$

(b) For Incident SV-Wave; $A^* = D_0$

$$[Y_1 = -a_{13}, \quad Y_2 = a_{23} \quad Y_3 = a_{33}, \quad Y_4 = -a_{43}, \quad Y_5 = a_{53}]$$

(c) For Incident T-Wave; $A^* = B_0$

$$[Y_1 = a_{12}, \quad Y_2 = -a_{22}, \quad Y_3 = -a_{32}, \quad Y_4 = a_{42}, \quad Y_5 = a_{52}]$$

The amplitude ratios Z_1, Z_2, Z_3 are for reflected P-, T- and SV-waves and Z_4, Z_5 are for transmitted P- and T-waves respectively.

(C): In absence of thermal effect in the thermally conducting liquid (Case **B**), we obtain the corresponding results at an interface of homogeneous inviscid liquid/thermoelastic solid half-spaces, yielding the four non-homogenous equations which can be presented as

(6.3)

$$\sum_{i=1}^{4} a_{ij} Z_j^* = Y_j^*, \quad (j = 1, 2, 3, 4),$$

where

$$a_{11} = iK_n\delta_1\sin\theta_1, \qquad a_{12} = iK_n\delta_2\sin\theta_2,$$

$$a_{13} = i\,K_n\delta_3\cos\theta_3, \qquad a_{14} = iK_n\delta_1'\sin\theta_1' + \lambda'\delta_1'^2,$$

$$a_{21} = -\left(\lambda + 2\mu\sin^2\theta_1\right)\delta_1^2 - \nu\,a_1, \qquad a_{22} = -\left(\lambda + 2\mu\sin^2\theta_2\right)\delta_2^2 - \nu\,a_2,$$

$$a_{23} = -\mu\delta_3^2\sin 2\theta_3, \qquad a_{24} = \lambda'\delta_1'^2,$$

$$a_{31} = \mu\delta_1^2\sin 2\theta_1, \qquad a_{32} = \mu\delta_2^2\sin 2\theta_2, \qquad a_{33} = \mu\delta_3^2\cos 2\theta_3, \qquad a_{34} = 0,$$

$$a_{41} = a_1\delta_1\sin\theta_1, \qquad a_{42} = a_2\delta_2\sin\theta_2, \qquad a_{43} = a_{44} = 0, \quad \text{[Insulated boundary]}$$

or

$$a_{41} = a_1, \qquad a_{42} = a_2, \qquad a_{43} = a_{44} = 0 \quad \text{[Isothermal boundary]},$$

where λ_1' and λ_2' are given by Eq. (6.2) with $c_1'^2 = \dfrac{\lambda'}{\rho'}$
and

$$Z_1^* = \frac{A_1}{A^*}, \qquad Z_2^* = \frac{B_1}{A^*}, \qquad Z_3^* = \frac{D_1}{A^*}, \qquad Z_4^* = \frac{A_1'}{A^*},$$

(a) For Incident P-wave; $A^* = A_0$

$$[Y_1^* = a_{11}, \qquad Y_2^* = -a_{21}, \qquad Y_3^* = a_{31}, \qquad Y_4^* = a_{41}]$$

(b) For Incident SV-wave; $A^* = D_o$

$$[Y_1^* = -a_{13}, \qquad Y_2^* = a_{23}, \qquad Y_3^* = -a_{33}, \qquad Y_4^* = a_{43}]$$

(c) For Incident T-wave; $A^* = B_o$

$$[Y_1^* = a_{12}, \qquad Y_2^* = -a_{22}, \qquad Y_3^* = a_{32}, \qquad Y_4^* = a_{42}]'$$

where Z_1^*, Z_2^*, Z_3^* are the amplitude ratios of reflected P- , T- and SV-waves respectively and Z_4^* is the amplitude ratio of a transmitted P-wave.

(D): Taking $\mu \to 0$ and $\mu' \to 0$ in medium M and M' respectively, we have thermally conducting liquid/thermally conducting liquid imperfect boundary and the corresponding results can be written as

(6.4) $$\sum_{i=1}^{4} a_{ij} Z_j^{**} = Y_j^{**}, \qquad (j = 1, 2, 3, 4),$$

where

$$a_{11} = iK_n\delta_1 \sin\theta_1, \qquad a_{12} = iK_n\delta_2 \sin\theta_2,$$

$$a_{13} = iK_n\delta'_1 \sin\theta'_1 + \lambda'\delta'^2_1 + \nu'a'_1, \qquad a_{14} = iK_n\delta'_2 \sin\theta'_2 + \lambda'\delta'^2_2 + \nu'a'_2,$$

$$a_{21} = a_1, \qquad a_{22} = a_2, \qquad a_{23} = -a'_1, \qquad a_{24} = -a'_2,$$

$$a_{31} = -\lambda\delta^2_1 - \nu\, a_1, \qquad a_{32} = -\lambda\delta^2_2 - \nu\, a_2,$$

$$a_{33} = \lambda'\delta'^2_1 + \nu'\, a'_1, \qquad a_{34} = \lambda'\delta'^2_2 + \nu'\, a'_2,$$

$$a_{41} = a_1\,\delta_1 \sin\theta_1, \qquad a_{42} = a_2\delta_2 \sin\theta_2,$$

$$a_{43} = -a'_1\delta'_1 \sin\theta'_1, \qquad a_{44} = -a'_2\delta'_2 \sin\theta'_2,$$

here

$$c_1^2 = \frac{\lambda}{\rho}, \qquad c'^2_1 = \frac{\lambda'}{\rho'}$$

and

$$Z_1^{**} = \frac{A_1}{A^*}, \qquad Z_2^{**} = \frac{B_1}{A^*}, \qquad Z_3^{**} = \frac{A'_1}{A^*}, \qquad Z_4^{**} = \frac{B'_1}{A^*},$$

(a) For Incident P-wave; $\mathrm{A}^* = A_0$

$$[Y_1^{**} = a_{11}, \qquad Y_2^{**} = -a_{21}, \qquad Y_3^{**} = -a_{31}, \qquad Y_4^{**} = a_{41}]$$

(b) For Incident T-wave; $A^* = B_0$

$$[Y_1^{**} = a_{12}, \qquad Y_2^{**} = -a_{22}^{**}, \qquad Y_3^{**} = -b_{32}^{**}, \qquad Y_4^{**} = a_{42}^{**}]$$

Z_1^{**}, Z_2^{**} are the amplitude ratios of reflected P- and T-waves and Z_3^{**}, Z_4^{**} are the amplitude ratios of the transmitted P- and T-waves respectively.

(E): In absence of the thermal effect in M and M' our results reduce to the interface of elastic and elastic half-spaces and are in agreement with the results if we solve the problem directly.

7. Particular cases

For deductions (A) and (E):
- $K_n \neq 0$, $K_t \to \infty$, corresponds to the case of normal stiffness boundary.
- Considering $K_n \to \infty$, $K_t \neq 0$, the results discussed above reduce to transverse stiffness boundary.
- Also taking $K_n \to \infty$, $K_t \to 0$, the corresponding results reduce to slip boundary.
- If we take $K_n \to \infty$, $K_c \neq 0$, then we obtain the corresponding results for a welded boundary.

For deductions (B), (C) and (D):

- $K_n \neq 0$, corresponds to the case of normal stiffness boundary.
- If we take $K_n \rightarrow \infty$, we obtain the corresponding results for a welded boundary.

8. Numerical results and discussion

With the view of illustrating the theoretical results obtained in the preceding sections and comparing these in various situations, we now present some numerical results. The materials chosen for this purpose are Magnesium (M) and Zinc (M'). Physical data of these metals are given (DHALIWAL and SINGH [11]) below:

Magnesium

$$\lambda = 2.696 \times 10^{10} \quad \text{Nm}^{-2},$$

$$\mu = 1.639 \times 10^{10} \quad \text{Nm}^{-2},$$

$$\rho = 1.74 \times 10^3 \quad \text{Kgm}^{-3},$$

$$C^* = 1.04 \times 10^3 \quad \text{JKg}^{-1} \text{ deg}^{-1},$$

$$\nu = 2.68 \times 10^6 \quad \text{Nm}^{-2} \text{ deg}^{-1},$$

$$T_0 = 298 \, \text{K},$$

Zinc

$$\lambda' = 8.58 \times 10^{10}, \quad \text{Nm}^{-2},$$

$$\mu' = 3.85 \times 10^{10}, \quad \text{Nm}^{-2},$$

$$\rho' = 7.14 \times 10^3 \quad \text{Kgm}^3,$$

$$C^{*'} = 3.9 \times 10^2 \quad \text{JKg}^{-1} \text{ deg}^{-1},$$

$$\nu' = 5.75 \times 10^6 \quad \text{Nm}^{-2} \text{deg}^{-1},$$

$$T_0' = 296 \, \text{K},$$

with the dimensionless value of $\dfrac{\omega}{\omega^{*'}} = 10$ and $\omega^* = \dfrac{4 \times C_1'}{\ell}$, where ℓ is the characteristic length and $\ell = 1$, $\dfrac{K_n}{\mu'\delta_1'} = 0.05$, $\dfrac{K_t}{\mu'\delta_1'} = 0.01$, $\dfrac{K_c}{K^{*'}\delta_1'} = 2$.

The material characteristic constant K^* has been selected at random. Thus for the non-dimensional quantity $C_T^2 = \dfrac{K^*}{\rho C^* C_1^2}$, we have taken the hypothetical value of $C_T = 0.5$. For this choice of material parameter in medium M, we have $K^* = \dfrac{C^*(\lambda + 2\mu)}{4}$. Similarly we select $K^{*'} = \dfrac{C^{*'}(\lambda' + 2\mu')}{4}$ for medium M'.

A computer programme has been developed and amplitude ratios of various reflected and transmitted waves have been computed. The variations of amplitude ratios for thermoelastic solid with Stiffness (ST), thermoelastic solid with Normal Stiffness (NS), thermoelastic solid with Transverse Stiffness (TS), thermoelastic solid with Thermal Contact Conductance (TCC) and thermoelastic solid with Welded Contact (WC) have been shown by solid line, dashed line, dashed line with central symbol 'circle', dashed line with central symbol 'triangle' and dashed line with central symbol 'cross' respectively. The variations of the amplitude ratios $|Z_i|$, $(i = 1, ..., 6)$ of various reflected and transmitted waves for ST, NS, TS, TCC and WC with angle of emergence θ_0 of different cases of the incident wave (P-, SV- or T-) have been shown in the Figs. 2–19.

Incident P-wave

The variations of amplitude ratios of the reflected and transmitted waves with angle of emergence from different boundaries for incident P-wave have been shown in Figs. 2–7.

Figure 2 shows the variation of amplitude ratios of the reflected P-wave with angle of emergence from various boundaries. It is evident that the values of amplitude ratio $|Z_1|$ for NS, TCC and WC is always greater than ST for all values of θ_0. The values of amplitude ratio $|Z_1|$ for TS are greater when $3° \leq \theta_0 \leq 18°$, $21° \leq \theta_0 \leq 46°$, $49° \leq \theta_0 \leq 90°$ and smaller for other values of θ_0 in comparison to ST. To present the variations clearly we have magnified the values of amplitude ratios for ST and TS by multiplying their original values by 10.
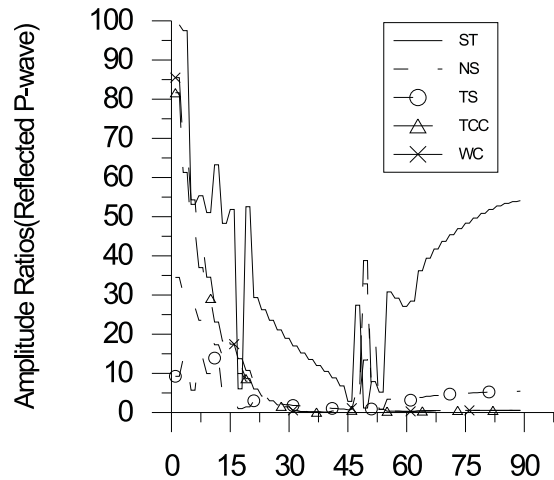
Fig. 2. Angle of Emergence (in deg.).

Figure 3 presents the variation of amplitude ratios of the reflected T-wave with angle of emergence from various boundaries. It is observed that the values of amplitude ratio $|Z_2|$ for NS, TCC and WC are greater than that of ST when $0° \leq \theta_0 \leq 26°$ and $49° \leq \theta_0 \leq 90°$. The values of amplitude ratio $|Z_2|$ for TS are greater when $0° \leq \theta_0 \leq 34°$ and smaller when $35° \leq \theta_0 \leq 90°$ in comparison to ST. The amplitude ratios for TCC and WC are equal for $55° \leq \theta_0 \leq 90°$.
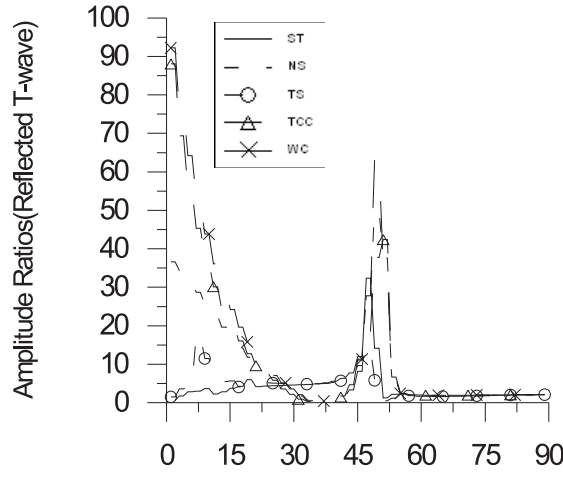
Fig. 3. Angle of Emergence (in deg.).

The variations of amplitude ratios of the reflected SV-wave with angle of emergence from various boundaries is shown by Fig. 4. The values of amplitude ratio $|Z_3|$ for NS is greater when $0° \leq \theta_0 \leq 18°$, $45° \leq \theta_0 \leq 54°$; for TS it
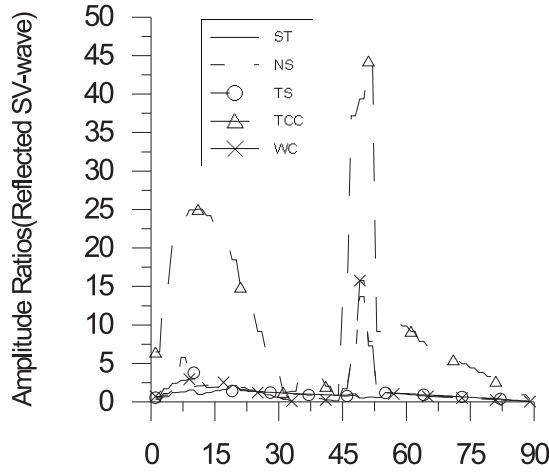
Fig. 4. Angle of Emergence (in deg.).

is greater when $0° \leq \theta_0 \leq 26°$, $77° \leq \theta_0 \leq 90°$; for TCC it is greater when $0° \leq \theta_0 \leq 22°$, $45° \leq \theta_0 \leq 54°$; for WC it is greater when $0° \leq \theta_0 \leq 24°$, $45° \leq \theta_0 \leq 54°$ and smaller for other ranges θ_0 in comparison to ST. In order to present the variations clearly we have magnified the values of amplitude ratios for TCC by multiplying their original value by 10.

Figure 5 shows the variations of amplitude ratios of transmitted P-wave with angle of emergence from various boundaries. It is seen that the value of amplitude ratio $|Z_4|$ for NS is greater than that of ST when $0° \leq \theta_0 \leq 38°$; $47° \leq \theta_0 \leq 52°$ and $55° \leq \theta_0 \leq 62°$ and is smaller for the other ranges. The value of amplitude ratio $|Z_4|$ for TCC and WC is greater when $0° \leq \theta_0 \leq 36°$; $47° \leq \theta_0 \leq 52°$ and smaller for the other ranges in comparison to that of ST respectively. Here the original value for TS is multiplied by 10.
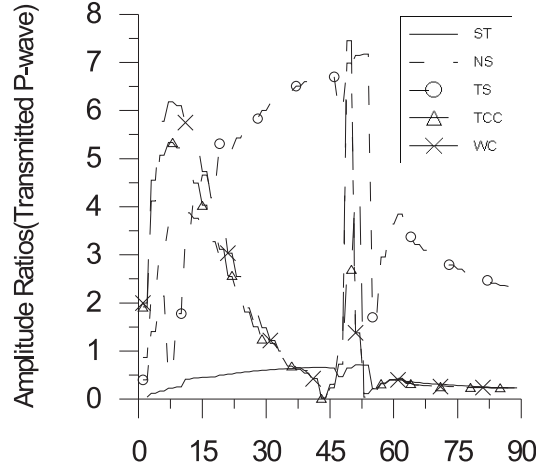
Fig. 5. Angle of Emergence (in deg.).

Figure 6 depicts the variation of amplitude ratios of a transmitted T-wave with angle of emergence. It is evident that the values of amplitude ratio $|Z_5|$ for TCC and WC are always greater than those of ST for all the values of θ_0. The values of amplitude ratio $|Z_5|$ for NS it is greater when $0° \leq \theta_0 \leq 56°$; $63° \leq \theta_0 \leq 90°$; for TS is greater when $55° \leq \theta_0 \leq 90°$ and smaller for the other ranges of θ_0 than that of ST. To depict the variations clearly we have magnified the values of amplitude ratios for ST and TS by multiplying their original value by 10.

The values of amplitude ratios of $|Z_6|$ (transmitted SV-waves) from various boundaries oscillates as a function of the angle of emergence and the variations is depicted by Fig. 7.
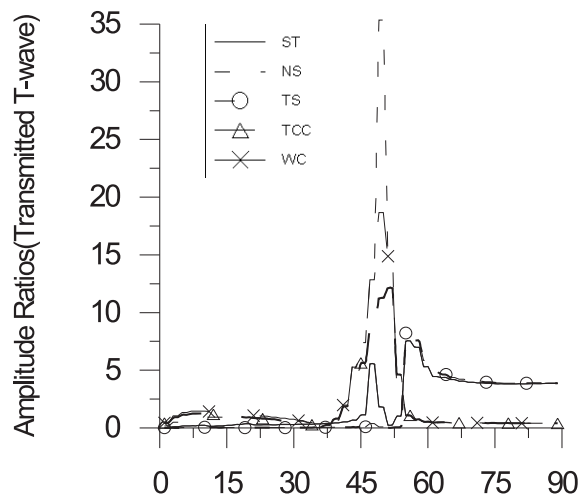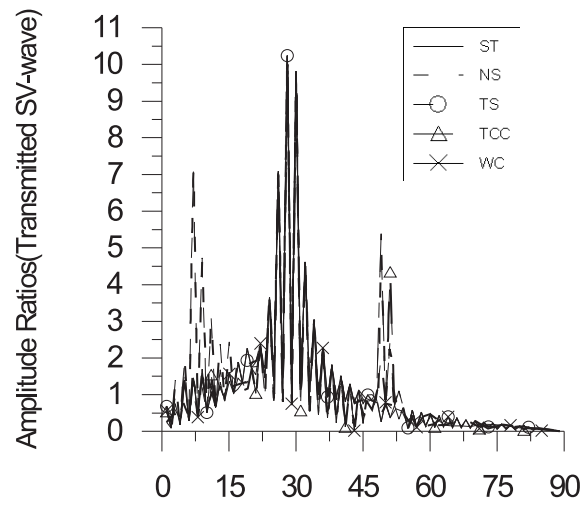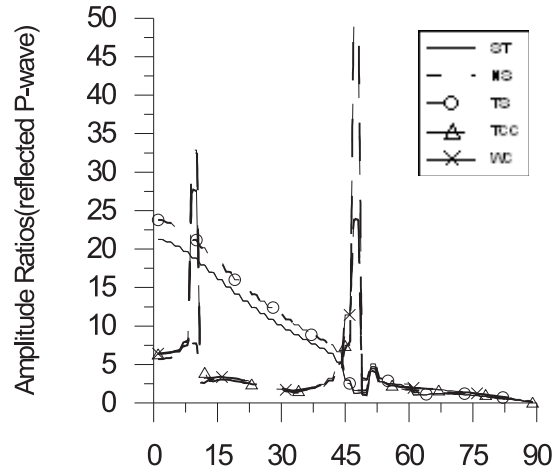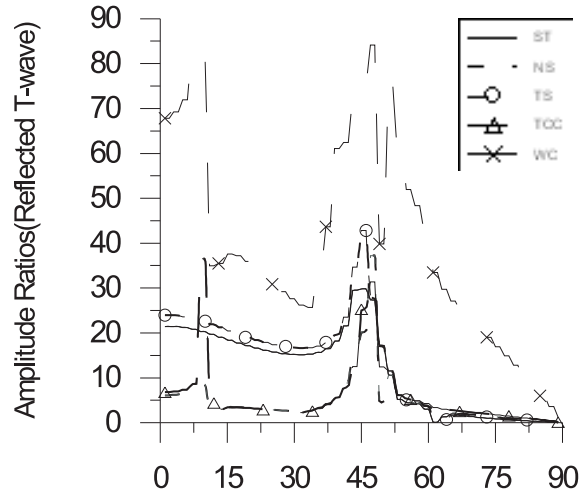
Fig. 6.   Angle of Emergence (in deg.).

Fig. 7.   Angle of Emergence (in deg.).

Incident SV-wave

The variation of amplitude ratios of various reflected and transmitted waves with angle of emergence when a SV-wave is incident, have been shown in Figs. 8–13.

Figure 8 shows the variation of amplitude ratios of the reflected P-wave with angle of emergence from various boundaries. It is evident that the values of

amplitude ratio $|Z_1|$ for NS are greater when $0° \leq \theta_0 \leq 44°$, $49° \leq \theta_0 \leq 60°$, $71° \leq \theta_0 \leq 90°$ and smaller for the other ranges of θ_0 in comparison to ST. The values of amplitude ratio $|Z_1|$ for TCC and WC are greater when $9° \leq \theta_0 \leq 10°$; $45° \leq \theta_0 \leq 52°$; $61° \leq \theta_0 \leq 90°$ and smaller for the other ranges of θ_0 in comparison to ST. It is clear that the value of amplitude ratio $|Z_1|$ for TS is always smaller than that of ST.

FIG. 8. Angle of Emergence (in deg.).

Figure 9 depicts the variations of amplitude ratios of the reflected T-wave with angle of emergence. It is observed that the values of amplitude ratio $|Z_2|$

FIG. 9. Angle of Emergence (in deg.).

for NS is greater when $51° \leq \theta_0 \leq 90°$; for TS it is greater when $0° \leq \theta_0 \leq 62°$, $67° \leq \theta_0 \leq 90°$; for TCC and WC it is greater when $9° \leq \theta_0 \leq 10°$, $47° \leq \theta_0 \leq 90°$ and smaller for the other ranges of θ_0 in comparison to that of ST. To depict the variations clearly we have magnified the value of amplitude ratios for WC by multiplying its original value by 10.
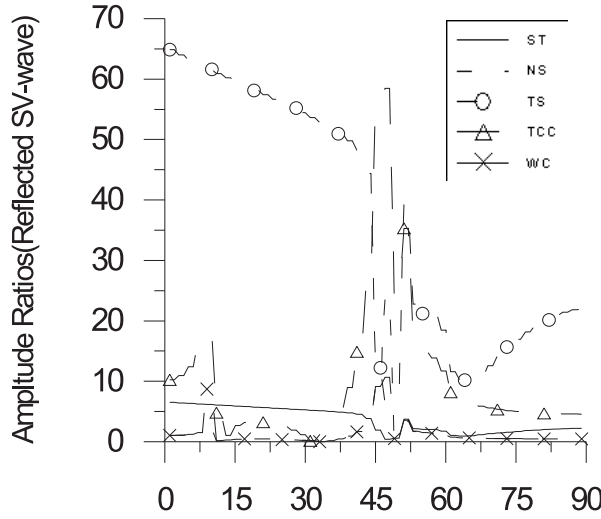
Figure 10 shows the variations of amplitude ratio $|Z_3|$ for a reflected SV-wave. It is evident that the value of amplitude ratio $|Z_3|$ is greater for NS and TCC when $45° \leq \theta_0 \leq 50°$; for TS when $7° \leq \theta_0 \leq 90°$; for WC when $9° \leq \theta_0 \leq 10°$, $47° \leq \theta_0 \leq 48°$ and smaller for the remaining values of θ_0 than that of ST. To depict the variations clearly we have magnified the value of amplitude ratios for TS and TCC by multiplying their original value by 10.

FIG. 10.   Angle of Emergence (in deg.).

Figure 11 shows the variations of amplitude ratios $|Z_4|$ of a transmitted P- wave. It is observed that the value of amplitude ratio $|Z_4|$ for NS, TCC and WC is greater when $43° \leq \theta_0 \leq 50°$, $61° \leq \theta_0 \leq 90°$ and for TS it is greater when $5° \leq \theta_0 \leq 44°$, $51° \leq \theta_0 \leq 90°$ and smaller for the remaining ranges of θ_0 than that of ST. To depict the variations clearly we have magnified the value of amplitude ratios for TS and WC by multiplying their original value by 10.

Figure 12 presents the variations of amplitude ratios $|Z_5|$ of a transmitted T-wave. It is observed that the value of amplitude ratio $|Z_5|$ for NS, TCC and WC is greater when $0° \leq \theta_0 \leq 70°$ and smaller for the remaining range of θ_0 than that of ST. It is clear that the amplitude ratio $|Z_5|$ for TS is always smaller

than that of ST. To depict the variations clearly we have magnified the values
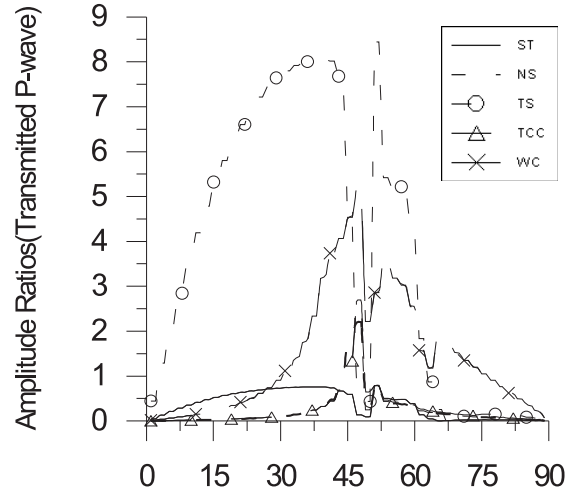of amplitude ratios for TS by multiplying their original value by 10.

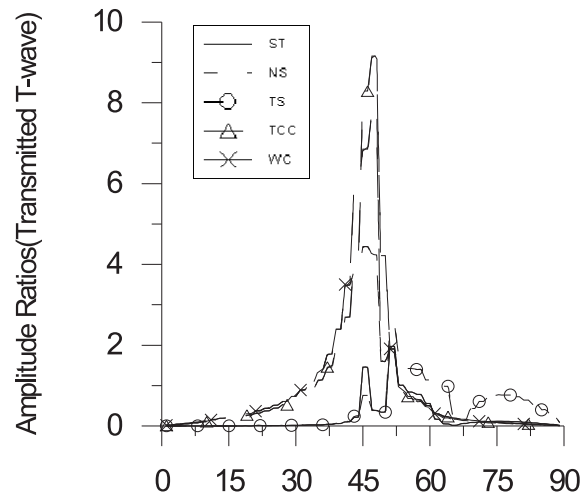Fig. 11. Angle of Emergence (in deg.).

Fig. 12. Angle of Emergence (in deg.).

Figure 13 shows the variations of a transmitted SV-wave. It is evident that
the values of amplitude ratio $|Z_6|$ oscillate as a function of the angle of emergence.
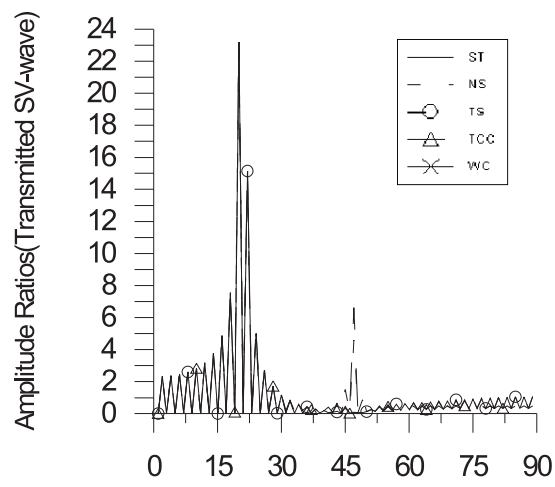
FIG. 13. Angle of Emergence (in deg.).

Incident T-wave

The variations of amplitude ratio of the reflected and transmitted waves with warying angle of emergence when T-wave is incident, is shown in Figs. 14–19.

Figures 14 and 15 show the variation of the amplitude ratios $|Z_1|$ and $|Z_2|$ of reflected P- and T-wave from various boundaries. It is observed that the value of the amplitude ratios of the waves for NS, TS, TCC and WC is always coincident with that of ST. To depict the variations, the amplitude ratios for TS and TCC are magnified by multiplying their original values by 10, whereas the amplitude ratios for NS and WC are divided by 10.
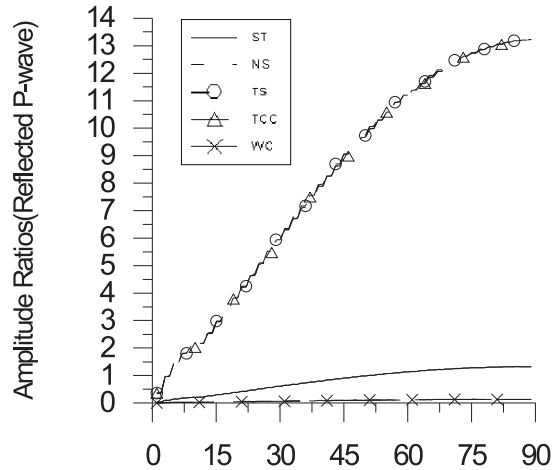

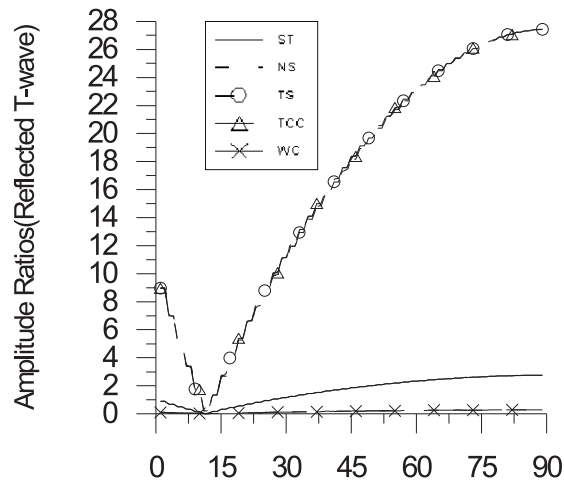FIG. 14. Angle of Emergence (in deg.).

FIG. 15. Angle of Emergence (in deg.).

Figure 16 depicts the variation of amplitude ratio $|Z_3|$ of a reflected SV-wave. It is evident that values of amplitude ratio for the other boundaries are always smaller in comparison with that of ST. Here we have divided the value of amplitude ratios for WC by 10, in order to depict the variations clearly.
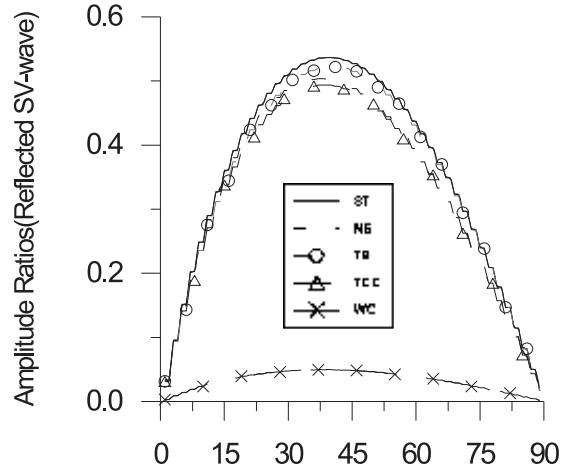

FIG. 16. Angle of Emergence (in deg.).

Figure 17 shows the variation of amplitude ratio $|Z_4|$ of a transmitted P-wave. It is clear that the values of amplitude ratio for NS, TS, TCC and WC are always smaller for all values of θ_0 than that of ST. To depict the variations clearly we have divided the values of amplitude ratios for NS and TCC by 10.
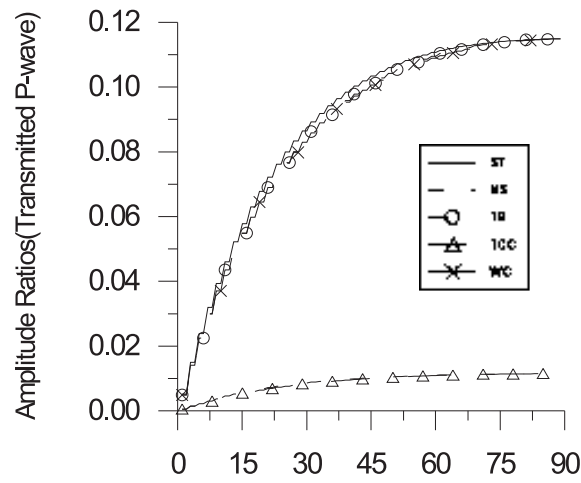
FIG. 17. Angle of Emergence (in deg.).

Figure 18 shows the variation of amplitude ratio $|Z_5|$ of a transmitted T-wave. The values of amplitude ratio for NS, TS, TCC and WC are always smaller for all values of θ_0 than that of ST. To depict the variations clearly we have divided the values of amplitude ratios for TS and WC by 10.
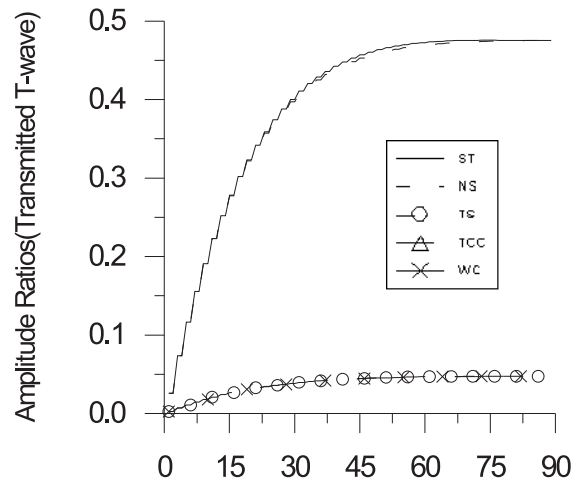

FIG. 18. Angle of Emergence (in deg.).

Figure 19 shows the variation of a transmitted SV-wave. It is clear that the values of amplitude ratio $|Z_6|$ oscillate as a function of the angle of emergence.
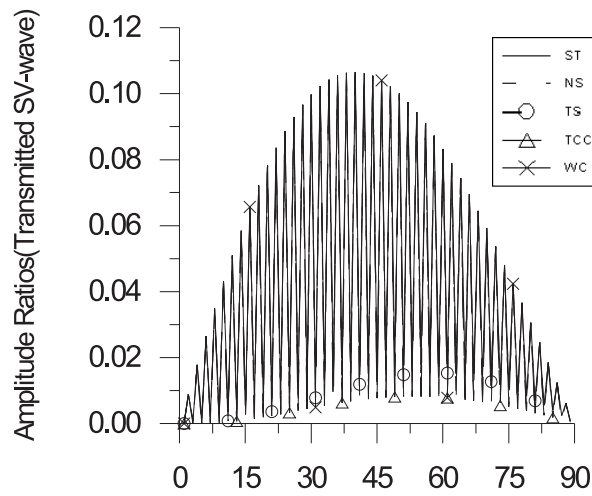
Fig. 19. Angle of Emergence (in deg.).

9. Conclusion

The thermoelastic theory developed by Green and Nagdhi [18] has been employed to study the problem. The analytical expressions of reflection and refraction coefficients of various reflected and refracted waves have been obtained for an imperfect, normal stiffness, transverse stiffness, thermally conducting, welded and slip boundaries. Some particular cases of interest have been deduced from the present investigation. It may be concluded that the thermal effect plays an important role on the reflection and refraction phenomenon. It is observed from the above figures that the behavior of the amplitude ratios is oscillatory in nature when P- or SV-wave is incident, whereas in the case when the T-wave is incident, the form of variations of the reflected P-, T- and SV-wave and the transmitted P- and transmitted T-wave is similar in nature for all the boundaries. The trend of variations of the transmitted SV-wave when either of the incident waves is oscillatory in nature. The model adopted in this paper is one of the most realistic forms of the earth model and it may be useful for experimental seismologists.

Acknowledgment

References

1. H. Deresiewicz, *Effect of boundaries on waves in a thermoelastic solid: Reflexion of plane waves from a plane boundary*, J. Mech. Phys. Solids, **8**, 164–172, 1960.

2. H. Deresiewicz, *Corrections and additions: Effect of boundaries on waves in a thermoelastic solid*, J. Mech. Phys. Solids, **10**, 179–181, 1962.

3. H.W. Lord and Y, Shulman, *A generalized dynamical theory of thermoelasticity*, J. Mech. Phys. Solids, **15**, 299–309, 1967.

4. J.P. Jones and J.P. Whittier *Waves in a flexible bonded interface*, J. Appl. Mech., **34**, 905–909, 1967.

5. A.E. Green and K.A. Lindsay, *Thermoelasticity*, J. Elasticity **2**, 1, 1–7, 1972.

6. A.N. Sinha and S.B. Sinha, *Reflection of thermoelastic waves at a solid half-space with thermal relaxation*, J. Phys. Earth, **22**, 237–244, 1974.

7. C.E. Beevers and J. Bree, *A note on wave reflection problems in linear thermoelasticity*, J. Math. Phys. Sci., **9**, 355–362, 1975

8. G.S. Murty *A theoretical model for the attenuation and dispersion of Stonley waves at the loosely bonded interface of elastic half-space*, Phys. Earth and Planetary Interiors, **11**, 65–79, 1975

9. A.H. Nayfeh and E.M. Nassar, *Simulation of the influence of bonding materials on the dynamic behaviour of laminated composites*, J. Appl. Mech., **45**, 855–828, 1978.

10. S.I. Rokhlin, M. Hefets and M. Rosen, *An elastic interface wave guided by a thin film between two solids*, J. Appl. Phys., **51**, 3579–3582, 1980.

11. R.S. Dhaliwal and A. Singh, *Dynamical coupled thermoelasticity*, Hindustan Publishers, Delhi, 1980.

12. S.I. Rokhlin, *Adhesive joint characterization by ultrasonic surface and interface waves*, Adhesive Joints: Formation, Characteristics and Testing. K.L. Mittal [Ed.], (Plenum, New York) 307–345, 1984.

13. J.M. Baik and R.B. Thompson *Ultrasonic scattering from imperfect interfaces a quasi-static model*, J. Nondestr. Eval., **4**, 177–196, 1984.

14. T.C. Angel and J.D. Achenbach, *Reflection and transmission of elastic waves by a periodic array of crack*, J. App. Mech., **52**, 33–41, 1985.

15. S.I. Rokhlin and D. Marom, *Study of adhesive bonds using low-frequency obliquely incident ultrasonic wave*, J. Acoust. Soc. Am., **80**, 585–590, 1986.

16. Pilarski and J.L. Rose, *A transverse wave ultrasonic oblique-incidence technique for interface weakness detection in adhesive bonds*, J. Appl. Phys., **63**, 300–307, 1988.

17. J.N. Sharma *Reflection of thermoelastic waves from the stress-free insulated boundary of an anisotropic half-space*, Indian J. Pure Appl. Math, **19**, 3, 294–304, 1988.

18. A.E. Green and P.M. Naghdi, *Thermoelasticity without energy dissipation*, Journal of elasticity, **31**, 189–208, 1993.

19. S. B. Sinha and K. A. Elasibai, *Reflection of thermoelastic waves at a solid half-space with two relaxation times*, J. Thermal Stresses, **19**, 749–762, 1996.

20. S. B. Sinha and K. A. Elasibai, *Reflection and Refraction of thermoelastic waves at an interface of two semi-infinite media with two relaxation times*, J. Thermal Stresses, **20**, 129–145, 1997.

21. A.I. Lavrentyev and S.I. Rokhlin, *Ultrasonic spectroscopy of imperfect contact interfaces between a layer and two solids*, J. Acoust. Soc. Am., **103**, 2, 657–664, 1998.

22. B. Singh and R. Kumar, *Reflection of plane waves from the flat boundary of a micropolar generalized thermoelastic half-space*, Int. J. Engng. Sci., **36**, 865–890, 1998.

23. B. Singh and R. Kumar, *Reflection of plane waves from the flat boundary of a micropolar generalized thermoelastic half-space with stretch*, Indian J. Pure Appl. Math., **29**, 6, 657–669, 1998.

24. B. Singh and R. Kumar, *Wave propagation in a generalized thermo-microstretch elastic solid*, Int. J. Engng. Sci., **36**, 891–912, 2003.

25. Abd-El-Nour, N. Abd-Alla and A.S Amira.Al-Dawy, *The reflection phenomena of SV-waves in generalized thermoelastic medium*, Int. J. Math and Math Sci., **23**, 8, 529–546, 2000.

26. B. Singh, *Wave propagation in an anisotropic generalized thermoelastic solid*, Indian J. pure Applied Math., **34**, 10, 1479–1485, 2003.

27. B. Singh, *Plane waves in a thermally conducting viscous liquid*, Sadhana, **29**, 1, 27–34, 2004.